

## Complete mapping of the tricuspid valve apparatus using three-dimensional sonomicrometry

Hosam Fawzy, MD,<sup>a</sup> Kiyotaka Fukamachi, MD, PhD,<sup>c</sup> C. David Mazer, MD,<sup>b</sup> Alana Harrington, MSc,<sup>b</sup> David Latter, MD,<sup>a</sup> Daniel Bonneau, MD,<sup>a</sup> and Lee Errett, MD<sup>a</sup>

**Objective:** Many surgeons consider the tricuspid valve to be a second-class structure. Our objective was to determine the normal anatomy and dynamic characteristics of the tricuspid valve apparatus in vivo and to discern whether this would aid the design of a tricuspid valve annuloplasty ring model.

**Methods:** Sixteen sonomicrometry crystals were placed around the tricuspid annulus, at the bases and tips of the papillary muscles, the free edges of the leaflets, and the right ventricular apex during cardiopulmonary bypass in 5 anesthetized York Hampshire pigs. Animals were studied after weaning of cardiopulmonary bypass on 10 cardiac cycles of normal hemodynamics.

**Results:** Sonomicrometry array localizations demonstrate the multiplanar shape of the tricuspid annulus. The tricuspid annulus reaches its maximum area ( $97.9 \pm 25.4 \text{ mm}^2$ ) at the end of diastole and its minimum area ( $77.3 \pm 22.5 \text{ mm}^2$ ) at the end of systole, and increases again in early diastole. Papillary muscles shorten by 0.8 to 1.5 mm (11.2%) in systole, and chordae tendineae straighten by 0.8 to 1.7 mm (11.4%) in systole.

**Conclusions:** The shape of the tricuspid annulus is a multiplanar 3-dimensional one with its highest point at the anteroseptal commissure and its lowest point at the posteroseptal commissure, and the anteroposterior commissure is in a middle plane in between. The tricuspid annulus area reaches its maximum during diastole and its minimum during systole. The papillary muscles contract by the same amount of chordal straightening. The optimal tricuspid annuloplasty ring may be a multiplanar 3-dimensional one that mimics the normal tricuspid annulus. (*J Thorac Cardiovasc Surg* 2011;141:1037-43)

The importance of the tricuspid valve is often overlooked by cardiologists and surgeons because of its unique characteristics. Most lesions of the tricuspid valve are not surgically corrected because of the incorrect assumption that tricuspid disease is rare and, in most cases, irrelevant to the patient's outcome after the problem in the left side of the heart that brings the patient to surgery has been solved.<sup>1-4</sup> This may be explained by the absence of a detailed preoperative study of the tricuspid valve.

A better understanding of the tricuspid valve is necessary to clarify the indications and limits of tricuspid valve surgery. Because of the importance of the annulus, an annulo-

plasty ring designed specifically for the tricuspid position should replicate the anatomy and function of the natural tricuspid valve as closely as possible. The specific geometric relationship that is formed by the attachment of the valve leaflets to the chordae tendineae, papillary muscles (PMs), and annulus is likely to be critical in ensuring proper function of both the valve and the right ventricle.<sup>5-8</sup>

This geometric relationship between components of the tricuspid valve, however, has not been studied in detail. Previous studies have documented that the mitral valve annulus is saddle shaped,<sup>9,10</sup> but how closely the tricuspid annulus (TA) resembles the mitral annulus and how the tricuspid annular shape changes during the cardiac cycle relative to contraction of the PMs has not been well studied. Because the annulus also has both fibrous and muscular components, it likely both dilates and contracts simultaneously within its various sections. Moreover, the network of supporting chordae is highly branched and complex, and the load distribution on these chordae also has not been studied. It is therefore unlikely that a successful tricuspid valve annuloplasty ring can be developed and properly implanted in patients unless a thorough understanding of the function of the tricuspid valve apparatus is obtained and implemented. Detailed spatial and temporal information is consequently needed to map the geometric and functional relationships among the contraction of the PMs, the stretching of the tricuspid valve chordae, and the distortion of the tricuspid valve annulus. Because of the unique

From the Division of Cardiovascular and Thoracic Surgery<sup>a</sup> and Departments of Anesthesia and Critical Care,<sup>b</sup> Keenan Research Centre in the Li Ka Shing Knowledge Institute, St Michael's Hospital, University of Toronto, Toronto, Ontario, Canada; and Department of Biomedical Engineering,<sup>c</sup> Lerner Research Institute, The Cleveland Clinic, Cleveland, Ohio.

Funding: Internal from the Division of Cardiovascular and Thoracic Surgery, St Michael's Hospital, University of Toronto, Toronto, Ontario, Canada.

Disclosures: Authors have nothing to disclose with regard to commercial support.

Oral presentation at the 62nd Annual Meeting of The Canadian Cardiovascular Society, October 24–28, 2009, Edmonton, Alberta, Canada.

Received for publication March 16, 2010; revisions received May 6, 2010; accepted for publication May 26, 2010; available ahead of print June 30, 2010.

Address for reprints: Hosam Fawzy, MD, Division of Thoracic and Cardiovascular Surgery, St. Michael's Hospital, 30 Bond Street, Toronto, Ontario, M5B 1W8 Canada (E-mail: fawzyh@smh.toronto.on.ca).

0022-5223/\$36.00

Crown Copyright © 2011 Published by Elsevier Inc. on behalf of The American Association for Thoracic Surgery

doi:10.1016/j.jtcvs.2010.05.039

### Abbreviations and Acronyms

3D	= 3-dimensional
PM	= papillary muscle
TA	= tricuspid annulus

characteristics of the tricuspid valve, it is called the “Cinderella” of the cardiac valves.<sup>3</sup>

The aim of this project was to study the anatomy and dynamic characteristics of the tricuspid valve apparatus using a porcine model. Better understanding of the normal anatomy and function of the tricuspid valve will help to clarify the indications and limits of tricuspid valve surgery.

### MATERIALS AND METHODS

The technique used in these studies was 16 channel 3-dimensional (3D) digital sonomicrometry (series 5001 digital sonomicrometer; Sonometrics Corp, London, Ontario, Canada). The sonomicrometer measures distances within soft tissue by means of piezoelectric transducers, a high-frequency counter, and the time of flight principle of ultrasound. Sixteen of these ultrasonic transducers were implanted into tissue (see below) and sequentially energized with a short electrical pulse. As each transducer was energized, it generated an acoustic wave that propagated through the tissue, away from the transducer in a radial manner. The method of 3D reconstruction and visualization was similar to that previously described.<sup>11</sup>

### Surgical Procedure

With the approval of the Institutional Animal Care and Use Committee, we developed a porcine model to study the anatomy and function of the tricuspid valve. We used 2- to 4-week-old Yorkshire pigs ( $n = 5$ ) with an average body weight of  $40.6 \pm 2$  kg. After cannulation of an ear vein, the animal was anesthetized with ketamine (20 mg/kg) and acepromazine (1 mg/kg). After endotracheal intubation, ventilation was controlled to maintain normocarbida with  $P_{aO_2}$  greater than 150 mm Hg. Anesthesia was maintained throughout the procedure with isoflurane or enflurane (1%–3%). An arterial cannula was inserted into the left external carotid artery for continuous blood pressure monitoring and arterial blood sampling for blood gases and serum electrolytes every 30 minutes. A pulmonary artery catheter was used to measure the pulmonary artery pressure. A right lateral thoracotomy followed by a pericardiectomy was performed to expose the heart and its great vessels. Heparin was given intravenously at the dose of 300 U/kg. Cannulation was carried out using an aortic cannula (Edwards Lifesciences G 22F; Irvine, CA) and 2 separate venous cannulae (Medtronic DLP size 28F; Minneapolis, MN) for the superior and inferior venae cavae. Once activated clotting time exceeded 480 seconds, cardiopulmonary bypass was started. The pump flow rate was 50 mL/kg/min (2–2.5 L/min). Temperature was kept at 32°C to 35°C (mild hypothermia) by drift. The aorta was then clamped, and cold blood cardioplegia (Fremes solution at 8:1 ratio and temperature of 4°C) was infused antegradely into the aortic root to stop the heart. Mean arterial pressure was maintained at 50 to 60 mm Hg throughout cardiopulmonary bypass. Transverse right atriotomy was performed to expose the tricuspid valve. The 16 sonomicrometer crystals were attached to the tricuspid valve apparatus as follows: Six crystals were placed at the base and apex of the 3 PMs, 2 for each one; 3 crystals were attached at the leaflet ends of the main marginal chordae at their sites of attachment to the anterior, posterior, and septal leaflets; 6 crystals were placed around the TA (3 at the commissures and 3 in between in the middle of annular attachment of each leaflet); and the remaining crystal was attached to the right ventricular apex as a reference (Figure 1). All the crystals

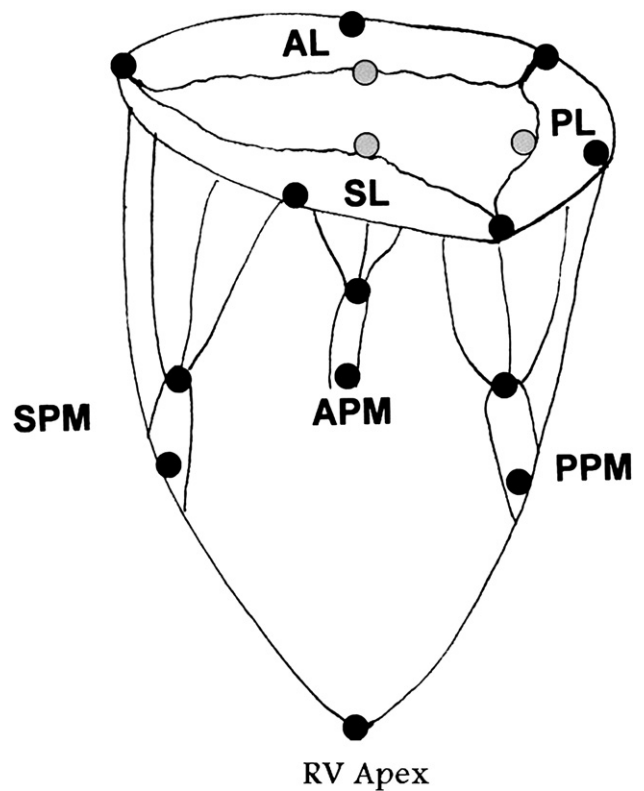


**FIGURE 1.** The positions of the crystals over the different parts of the tricuspid valve apparatus. *AL*, Anterior leaflet; *PL*, posterior leaflet; *SL*, septal leaflet; *APM*, anterior papillary muscle; *PPM*, posterior papillary muscle; *SPM*, septal papillary muscle; *RV Apex*, right ventricular apex.

were fixed using 5-0 Prolene sutures. The wires for the crystals fixed to the annulus and the chordae tendineae were routed through the atrium, and those fixed to the PMs were routed out through a small incision at the right ventricular apex. Each crystal was connected to the sonomicrometer, and the pig was weaned from cardiopulmonary bypass. Heparin reversal was achieved using intravenous protamine at a dose of 10 mg per 100 units of heparin. After hemodynamics reached the normal preoperative status, data were acquired for 5 to 10 consecutive cardiac cycles over a 5-second interval. At the end of the experiment, the animal was sacrificed by exsanguination into the cardiotomy reservoir.

### Data Analysis

All data from the individual outputs were imported into Excel worksheets (Microsoft Corp, Redmond, WA) for organizational purposes. For the isolated time period for the measured variables, maximum, minimum, difference, mean, and standard deviation were calculated. Data were expressed as mean  $\pm$  standard deviation and compared using 2-tailed unpaired Student *t* test.

### RESULTS

#### Model Characteristics

The hemodynamics at the time of recording were heart rate  $75 \pm 6$  beats/min, arterial pressure  $68/40 \pm 2/4$  mm Hg, and pulmonary artery pressure  $23/14 \pm 3/2$  mm Hg. All hemodynamic data are shown in Table 1. At necropsy, all transducers were in the correct positions in all the animals.

**TABLE 1. Hemodynamic data during recording**

Hemodynamic parameters	Pre-CPB	During recording	P value
Heart rate (beats/min)	78 ± 7	75 ± 6	NS
Systolic blood pressure (mm Hg)	67 ± 4	68 ± 2	NS
Diastolic blood pressure (mm Hg)	43 ± 2	40 ± 4	NS
Mean blood pressure (mm Hg)	51 ± 3	49 ± 3	NS
Systolic pulmonary pressure (mm Hg)	25 ± 6	23 ± 3	NS
Diastolic pulmonary pressure (mm Hg)	13 ± 4	14 ± 2	NS
Mean pulmonary pressure (mm Hg)	17 ± 5	17 ± 2	NS

CPB, Cardiopulmonary bypass; NS, not significant. Values are means ± standard deviation.

### Tricuspid Annulus Changes

Sonomicrometry array localizations demonstrate the multiplanar shape of the TA with its highest point at the antero-septal commissure and its lowest point at the posteroseptal commissure. The TA reaches its maximum area at the end of diastole and its minimum at the end of systole and increases again in early diastole. The PMs shorten in systole, and chordae tendineae straighten in systole.

**Two-dimensional shape of the tricuspid annulus.** The localized distances of each of the 6 crystals fixed to the TA from the reference crystal at the apex of the right ventricle are summarized in Figure 2. The posteroseptal segment of the TA was close to the right ventricular apex, and the lowest point was the posteroseptal commissure. In contrast, antero-septal and anteroposterior segments were close to the right atrium, and the highest point of the TA was at the antero-sep-

tal commissure. The anteroposterior commissure was at a plane in between the antero-septal and posteroseptal commissures.

**Three-dimensional shape of the tricuspid annulus.** The shape of the TA was determined by the 3D coordinates of each annulus crystal. Figure 3 is a comprehensive illustration of the 3D shape of TA at end systole from 1 animal. An arbitrary surface passing through each of the annular transducers has been drawn for better demonstration of the multi-planar shape of the annulus, which is maintained throughout the cardiac cycle. All pigs studied had annuli of similar shapes. The resultant averages determined a multi-planar-oriented shape with a highest point corresponding to the antero-septal crystal, an intermediate point corresponding to the anteroposterior crystal, and a lowest point corresponding to the posteroseptal crystal.

**Dynamic changes of the tricuspid annular area.** The tricuspid annular area increased from mid to late diastole, reaching a maximum area of  $97.9 \pm 25.4 \text{ mm}^2$  at the end of diastole; decreased during systole, reaching its minimum of  $77.3 \pm 22.5 \text{ mm}^2$  at the end of systole; and increased again in early diastole, showing a biphasic pattern with 2 peaks in early and late diastole (Figure 4).

**Dynamic changes of the tricuspid annular perimeter.** The TA perimeter was also calculated to measure the cross-sectional changes during different phases of the cardiac cycle. The annular perimeter expanded from a minimum of  $82.5 \pm 19.0 \text{ mm}$  in late systole to a maximum of  $89.0 \pm 19.2 \text{ mm}$  in late diastole with an expansion of  $7.9\% \pm 0.8\%$ . However, this total expansion was not homogenous in all segments. Most of the changes of the annular circumference were along the anterior annulus ( $16.2\% \pm 3.1\%$ ). As viewed in the axial plane (Figure 5), there was relatively

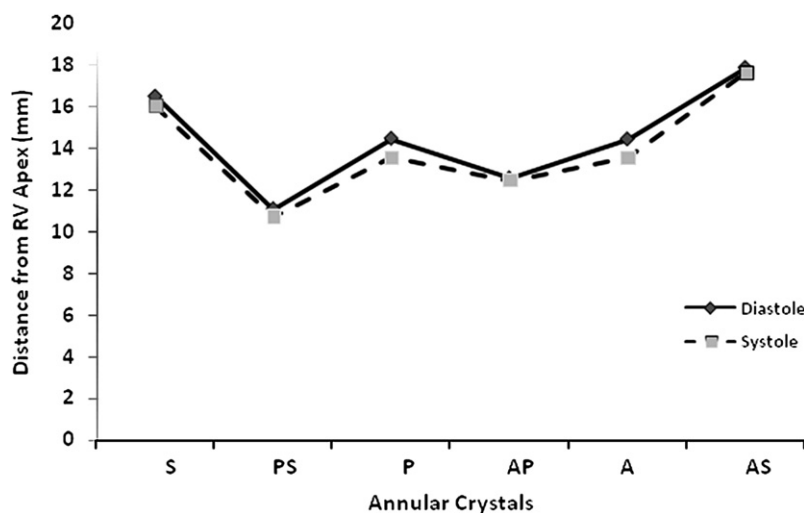


**FIGURE 2.** The distances of the 6 tricuspid annular crystals in relation to the right ventricular apex. S, Crystal at the middle of the septal annulus; PS, crystal at the posteroseptal commissure; P, crystal at the middle of the posterior annulus; AP, crystal at the anteroposterior commissure; A, crystal at the middle of the anterior annulus; AS, crystal at the antero-septal commissure.

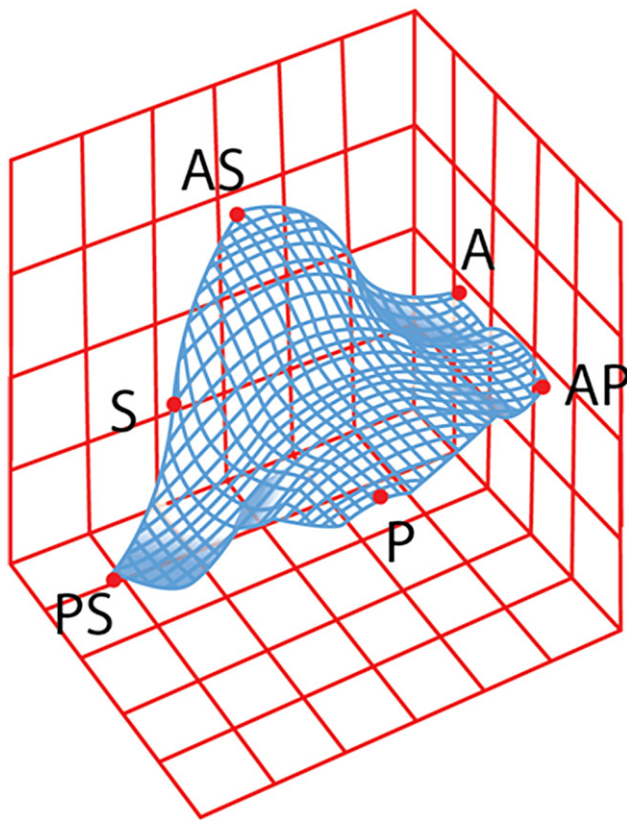


**FIGURE 3.** The 3D shape of the TA at systole. *S*, Crystal at the middle of the septal annulus; *PS*, crystal at the posteroseptal commissure; *P*, crystal at the middle of the posterior annulus; *AP*, crystal at the anteroposterior commissure; *A*, crystal at the middle of the anterior annulus; *AS*, crystal at the anterosseptal commissure.

little change of the circumference along the posterior annulus ( $12.5\% \pm 3.5\%$ ). The septal expansion was smaller ( $10.1\% \pm 0.9\%$ ) than that of the anterior or posterior segments, but not statistically significant ( $P = .28$  and  $P = .58$ , respectively). The changes of the different parts of the tricuspid valve apparatus are shown in [Table 2](#).

### Leaflet Motion

The opening area of the tricuspid valve leaflets was determined from the area of the triangles designated by the 3 crystals on the edges of the 3 leaflets and the 6 annular crystals. The leaflets began to open in early diastole, completing their opening by the end of diastole. This is followed by closure during ventricular systole. The maximum tricuspid leaflet area occurred near end systole and averaged  $127.3 \pm 33 \text{ mm}^2$ , and the minimum area occurred at the end of diastole and averaged  $100.5 \pm 29.3 \text{ mm}^2$ . The mean ratio of leaflet area to orifice area was 1.3.

### Chordae Tendineae

The distance between crystals on the chordae tendineae began to lengthen in early systole, reaching its maximum

by the end of systole and its minimum in diastole. The inter-crystal distance of the anterior chordae tendineae lengthened by  $14.0\% \pm 4.6\%$ , whereas that of the posterior chords increased by  $16.9\% \pm 8.4\%$  and that of the septal chords by  $5.2\% \pm 0.4\%$ . The overall chordal straightening was 11.4%.

### Papillary Muscle Movement

The motion of the PMs relative to the tricuspid annular plane can be described as a combination of shifting, twisting, and bending movements. During the cardiac cycle, the average of the 3 PMs contracted by 11.2% during systole and the maximum change in length was 0.8 to 1.5 mm.

The PMs were shortest during systole and longest during diastole. However, the torsion along the septal PM ( $16.2\% \pm 6.0\%$ ) was insignificantly greater in magnitude than anterior PMs ( $11.1\% \pm 1.3\%$ ,  $P = .35$ ) and significantly greater than posterior PMs ( $7.5 \pm 3.4$ ,  $P = .029$ ).

Angular displacement of the PMs below the corresponding commissures showed that the PMs did not move together in the same direction and the PM plane was not parallel to the TA plane. In fact, the angles between the 2 planes were 54.1 degrees, 66.4 degrees, and 41.7 degrees for anterior, posterior, and septal PMs, respectively.

### DISCUSSION

Because the majority of tricuspid valve pathology has been considered secondary to left-sided lesions and pulmonary hypertension, it has been assumed to revert spontaneously after these lesions have been treated. These factors, together with its characteristic paucity of clinical manifestations, have resulted in a lack of solid principals for tricuspid disease diagnosis, indications, and appropriate surgical maneuvers. The diagnostic and surgical methods for treating functional tricuspid regurgitation previously closely followed those applied for the mitral valve. However, the tricuspid valve has distinguishing characteristics that are not often appreciated. Moreover, a recent review of 790 patients who underwent different techniques of tricuspid annuloplasty showed that between 15% and 37% of these cases had recurrent severe regurgitation at 8 years follow-up.<sup>12</sup> These results suggest that the current annuloplasty techniques are unreliable or insufficient.

We demonstrated that the shape of the TA is multiplanar with non-homogenous contraction. The highest point of the TA is at the anterosseptal commissure. The lowest point is at the posteroseptal commissure. The geometry of the TA thus may be complicated and appears to be different from the saddle shape of the mitral annulus, suggesting an annuloplasty in tricuspid regurgitation should be different from that in mitral regurgitation. Fukuda and colleagues<sup>13</sup> studied the tricuspid valve in both healthy subjects and patients with tricuspid regurgitation using real-time 3D echocardiography and observed a TA shape similar to that in our study.

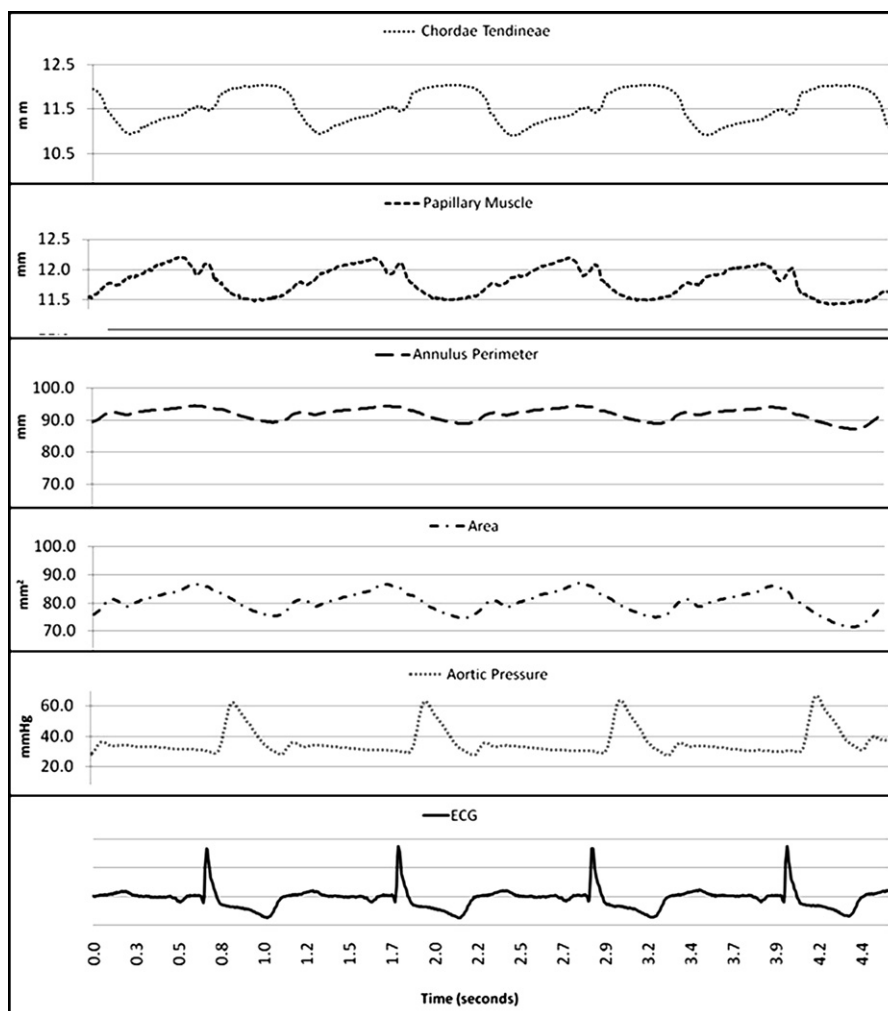


FIGURE 4. The dynamic changes of the tricuspid valve apparatus during the cardiac cycle in 1 animal.

There have been many studies of the saddle-shaped mitral annulus.<sup>14-16</sup> Many surgeons still believe that the TA has the same saddle shape of the mitral annulus. In a previous study with a small number of subjects, 3D echocardiography with reconstruction was used to measure the 3D structure of the normal TA and suggested that the TA is saddle shaped.<sup>17</sup> A recent experimental study used sonomicrometry in an ovine model with opening of the pericardium.<sup>18,19</sup> They described a saddle shape of the TA with the highest point corresponding to the midpoint of the posterior leaflet and the lowest point corresponding to the anteroposterior commissure. The anterosseptal commissure and the middle of the anterior leaflet are located in a middle plane.

In the postmortem human heart, Deloche and colleagues<sup>20</sup> described the shape of the normal TA as pear shaped with its narrow end at the anterosseptal commissure and its wider end at the midpoint of the posterior leaflet. The same pear-shaped annulus was also described by Hiro and colleagues<sup>18</sup> in their pressurized postmortem sheep heart. However, in

their recent *in vivo* ovine model, they observed the opposite shape with the narrow end of the pear-shaped annulus at the posteroseptal commissure.<sup>18</sup> This variation of the shape of the TA in different reports may be explained by different animal model used in each study.

The mechanical advantage of the saddle shape of the mitral annulus is well known because it has been shown to reduce valve stress.<sup>21</sup> These issues have not been fully studied for the TA.

The present study found that changes in the multiplanar shape of the TA during the cardiac cycle also contribute to its orifice area. The decrease in the multiplanar shape during systole has a “folding” reducing effect on the TA. This minimizes leaflet stress and allows a “folding” of the annulus that effectively reduces its orifice area without a dramatic reduction in perimeter. This change in shape is the main mechanism responsible for the TA competence and questions the efficiency of rigid annuloplasty devices that interfere with this mechanism. With an open heart dog model, Tsakiris

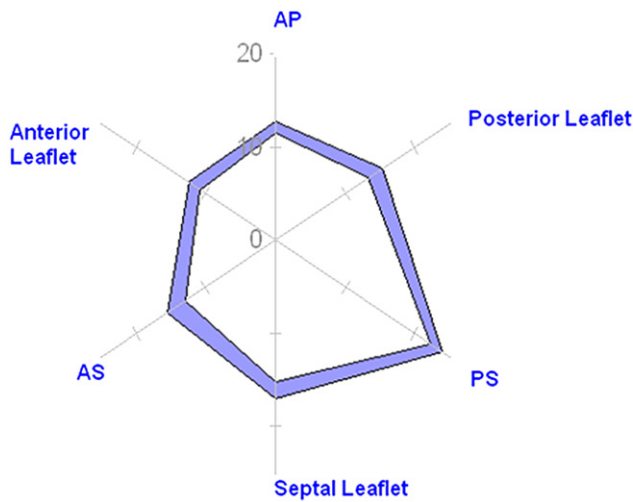


**FIGURE 5.** The segmental changes of different parts of the TA. PS, Postero-septal commissure; AP, anteroposterior commissure; AS, anteroseptal commissure.

and colleagues<sup>7</sup> found that the tricuspid valve is not a rigid structure with atrial and ventricular contractions that are responsible for TA competence, with the major part of annular narrowing caused by atrial contraction. Atrial contraction brought the anterior and posterior leaflets to appose the septal leaflet.

Previous experimental and clinical studies have shown that the TA continuously changes its size and shape during the cardiac cycle.<sup>7</sup> In the present study, the TA area contracted to 21% of its maximum area. These obtained data confirmed those of Tsakiris and associates,<sup>7</sup> who reported a contraction between 20% and 39% of the maximal diastolic area. In an echocardiographic study of normal humans, Tei and colleagues<sup>6</sup> showed a maximum reduction of 33%. An earlier report by Hiro and colleagues<sup>18</sup> showed that TA became less circular and decreased from  $0.55 \pm 0.05$  mm to  $0.46 \pm 0.04$  mm.

**TABLE 2.** Length data for tricuspid valve annulus, chordae tendineae, and papillary muscles

Measurement	Minimum (mm)	Maximum (mm)	Change (%)
<b>Annulus</b>			
Anterior segment	$11.6 \pm 1.1$	$13.5 \pm 1.7$	$16.2\% \pm 3.1\%$
Posterior segment	$15.5 \pm 5.7$	$17.3 \pm 5.7$	$12.5\% \pm 3.5\%$
Septal segment	$16.7 \pm 5.1$	$18.7 \pm 4.4$	$10.1\% \pm 0.9\%$
<b>Chordae tendineae</b>			
Anterior chord	$9.6 \pm 3.1$	$11.0 \pm 3.1$	$14.0\% \pm 4.6\%$
Posterior chord	$9.5 \pm 3.3$	$11.2 \pm 2.8$	$16.9\% \pm 8.4\%$
Septal chord	$14.0 \pm 3.5$	$14.8 \pm 3.7$	$5.2\% \pm 0.4\%$
<b>Papillary muscles</b>			
Anterior PM	$11.8 \pm 2.6$	$13.3 \pm 3.1$	$11.1\% \pm 1.3\%$
Posterior PM	$11.0 \pm 4.0$	$11.8 \pm 3.9$	$7.5\% \pm 3.4\%$
Septal PM	$6.5 \pm 1.7$	$7.6 \pm 1.4$	$16.2\% \pm 6.0\%$

PM, Papillary muscle. Values are means  $\pm$  standard deviation.

However, these changes were not homogenous in all segments. Most of the changes of the annular circumference were along the anterior annulus and then the posterior annulus, whereas the least reduction occurred at the septal segment with no significant difference. Hiro and colleagues<sup>18</sup> reported that the length of insertion of the septal leaflet changed almost as much as the insertion of the anterior and posterior leaflets ( $10.4\% \pm 1.2\%$  vs  $13.0\% \pm 1.5\%$  vs  $14.0\% \pm 1.6\%$ , respectively). They showed that the reduction in the annulus orifice was due to a selective shortening of the free wall portions.

The biphasic nature of the TA area curve is comparable to that observed in the mitral valve by Gorman and colleagues<sup>9</sup> and in the tricuspid valve by Tei and colleagues<sup>6</sup> and Tamiya and colleagues.<sup>22</sup> The maximum TA area occurred during late diastole and is most likely due to relaxation of the right ventricular transverse fibers in late diastole.<sup>23</sup>

The PMs contracted by 11.2%, and the chordae tendineae straightened by 11.4%. This has not been reported previously and suggests that there is a balance between active structures that contract and passive structures that expand, producing minimal geometric distortion of the tricuspid valve apparatus.

The length of the tricuspid valve's septal segment also changes during the cardiac cycle ( $10.1\% \pm 0.9\%$ ). This finding challenges both the standard method of using the length of the septal leaflet base to select the correct ring size and the use of open annuloplasty bands, which may not prevent further dilatation of the diseased TA. Using the length of the base of the septal leaflet to determine the optimal size of the repaired annulus was derived from the mitral valve, where the fibrous intertrigonal segment was considered stable and constant.

On the basis of the current understanding of the 3D geometry of the normal TA, we suggest a new 3D design for a tricuspid annuloplasty ring that is not a saddle shape but instead is multiplanar 3D in shape, with its highest point at the anteroseptal commissure and its lowest point at the postero-septal commissure, while the anteroposterior commissure lies in a middle plane in between (Figure 6) (patent pending). Such a tricuspid annuloplasty ring may be made from a semi-rigid material that does not interfere with the folding mechanism of the annulus. The material may have a progressive degree of flexibility along the whole length of the ring from septal through the posterior and anterior segments. The ring may have its lowest flexibility near the septal leaflet and the highest flexibility near the anterior leaflet.

**Study Limitations**

The number of the animals used in this study was small. Intraoperative echocardiography might have helped in confirming the positions of the crystals and excluding any potential effects of the crystals on the tricuspid valve motions and any possible tricuspid valve regurgitation. However,



**FIGURE 6.** The proposed tricuspid annuloplasty ring.

shadowing from the crystals may have precluded such assessments. Finally, by aiming to study the normal anatomy and physiology of the normal tricuspid valve, we did not compare any annuloplasty devices that could be explored in detail in future studies using the same sonomicrometry technology and a larger number of animals.

## CONCLUSIONS

The tricuspid valve apparatus is a complex structure with an efficient valvular mechanism and geometry that change continuously during the cardiac cycle. The shape of the TA is not a saddle shape. The TA has a multiplanar 3D shape with its highest point at the antero-septal commissure and its lowest point at the postero-septal commissure, and the antero-posterior commissure is in a middle plane in between. The TA area undergoes 2 major contraction and expansions during the cardiac cycle, reaching its maximum during diastole and its minimum during systole. The PMs contract by the same amount of chordal straightening. This suggests there is a balance between active structures that contract and passive structures that expand, producing minimal geometric distortion of the tricuspid apparatus. The optimal tricuspid annuloplasty ring may be a multiplanar 3D one that mimics the normal anatomic shape of the TA.

## References

- Duran CM, Pomar JL, Colman T, Figueroa A, Revuelta JM, Ubago JL. Is tricuspid valve repair necessary? *J Thorac Cardiovasc Surg.* 1980;80:849-60.
- Carpentier A, Deloche A, Dauptain J, et al. A new reconstructive operation for correction of mitral and tricuspid insufficiency. *J Thorac Cardiovasc Surg.* 1971;61:1-13.
- Duran CM. Acquired disease of the tricuspid valve: In: *Gibbon's Surgery of the Chest.* Section II, 7th ed. Philadelphia: Elsevier; 2005:1335-54.
- Angermann CE, Spes CH, Tammen A, et al. Anatomic characteristics and valvular function of the transplanted heart: transthoracic versus transesophageal echocardiographic findings. *J Heart Transplant.* 1990;9:331-8.
- Ohata T, Kigawa I, Tohda E, et al. Comparison of durability of bioprosthesis in tricuspid and mitral position. *Ann Thorac Surg.* 2001;71:S240-3.
- Tei C, Pilgrim JP, Shah PM, et al. The tricuspid valve annulus: study of size and motion in normal subjects and in patients with tricuspid regurgitation. *Circulation.* 1982;66:665-71.
- Tsakiris AG, Mair DD, Seki S, et al. Motion of the tricuspid valve annulus in anesthetized intact dogs. *Circ Res.* 1975;36:43-8.
- Munro AI, Jamieson WRE, Tyers GFO, et al. Tricuspid valve replacement: porcine bioprosthesis and mechanical prosthesis. *Ann Thorac Surg.* 1995;59: S470-1.
- Gorman JH III, Gupta KB, Streicher JT, et al. Dynamic three-dimensional imaging of the mitral valve and left ventricle by rapid sonomicrometry array localization. *J Thorac Cardiovasc Surg.* 1996;112:712-26.
- Cheng TO, Xie MX, Wang XF, Li ZA, Hu G. Evaluation of mitral valve prolapse by four dimensional echocardiography. *Am Heart J.* 1997;133:120-9.
- Vesely I, Fawzy H, Fukamachi K, Drake M. Use of three-dimensional sonomicrometry to study the motion of the mitral valve. *ASAIO J.* 1997;43:M465-9.
- McCarthy PM, Bhudia SK, Rajeswaran J, et al. Tricuspid valve repair: durability and risk factors for failure. *J Thorac Cardiovasc Surg.* 2004;127:674-85.
- Fukuda S, Saracino G, Matsumura Y, et al. Three-dimensional geometry of the tricuspid annulus in healthy subjects and in patients with functional tricuspid regurgitation, a real-time 3-dimensional echocardiographic study. *Circulation.* 2006;114(suppl 1):I-492-8.
- Levine RA, Handschumacher MD, Sanfilippo AJ, et al. Three-dimensional echocardiographic reconstruction of the mitral valve, with implications for the diagnosis of mitral valve prolapse. *Circulation.* 1989;80:589-98.
- Glasson JR, Komeda MK, Daughters GT, et al. Three-dimensional regional dynamics of the normal mitral annulus during left ventricular ejection. *J Thorac Cardiovasc Surg.* 1996;111:574-85.
- Kwan J, Qin JX, Popovic ZB, Agler DA, Thomas JD, Shiota T. Geometric changes of mitral annulus assessed by real-time 3-dimensional echocardiography: becoming enlarged and less nonplanar in the anteroposterior direction during systole in proportion to global left ventricular systolic function. *J Am Soc Echocardiogr.* 2004;17:1179-84.
- Chandra S, Powell K, Breburda CS, et al. Three dimensional reconstruction (shape and motion) of tricuspid annulus in normals and in patients after tricuspid annuloplasty with a flexible ring. *Comput Cardiol.* 1996;23:693-6.
- Hiro ME, Jouan J, Pagel MR, et al. Sonometric study of the normal tricuspid valve annulus in sheep. *J Heart Valve Dis.* 2004;13:452-60.
- Jouan J, Pagel MR, Hiro ME, Lim KH, Lansac E, Duran CMG. Further information from sonometric study of the normal tricuspid valve annulus in sheep: geometric changes during the cardiac cycle. *J Heart Valve Dis.* 2007;16:511-8.
- Deloche A, Guerinon J, Fabiani JN, et al. [Anatomical study of rheumatic tricuspid valvulopathies. Applications to the critical study of various methods of annuloplasty]. *Arch Mal Coeur Vaiss.* 1974;67:497-505 (in French).
- Salgo IS, Gorman JH 3rd, Gorman RC, et al. Effect of annular shape on leaflet curvature in reducing mitral leaflet stress. *Circulation.* 2002;106:711-7.
- Tamiya K, Higashidate M, Kikkawa S. Real-time and simultaneous measurement of tricuspid orifice and tricuspid annulus areas in anesthetized dogs. *Circ Res.* 1989;64:427-36.
- Coghlan C, Prieto G, Harrison TR. Movement of the heart during the period between the onset of ventricular excitation and the start of left ventricular ejection. *Am Heart J.* 1961;62:65-82.